JOURNAL OF CATALYSIS **157**, 368–379 (1995)

Vanadia Catalysts Supported on Mixed TiO_2–Al_2O_3 Supports: Effect of Composition on the Structure and Acidity

H. K. Matralis,[1] M. Ciardelli, M. Ruwet, and P. Grange

Catalyse et Chimie des Materiaux Divises, Universite Catholique de Louvain, Place Croix du Sud 2/17, 1348 Louvain-la-Neuve, Belgium

Received November 7, 1994; revised June 1, 1995; accepted July 26, 1995

Two series of V_2O_5/TiO_2–Al_2O_3 catalysts were prepared. In the first, a constant loading of vanadium (7.5 wt% V_2O_5) was deposited on a series of mixed TiO_2–Al_2O_3 supports of various compositions (0–82 wt% Al_2O_3), whereas in the second series various amounts of vanadium (4.5–10.5 wt% V_2O_5) were supported on a TiO_2–10 wt% Al_2O_3 support. X-ray diffraction analysis (XRD), X-ray photoelectron spectroscopy (XPS), and IR spectroscopy were used to study the influence of the composition on the structure of the catalysts and on the oxidation state of supported vanadium species. The acidity of the catalysts was studied using IR of chemisorbed NH_3. The results showed the presence of surface V^{4+} species, in addition to V^{+5} species, on the V_2O_5/TiO_2–Al_2O_3 catalysts. The ratio V^{4+}/V^{5+} was found to depend strongly on both the composition of the mixed support and the loading of vanadium. Deposition of vanadium on these mixed carriers results in an increase of the strength of Lewis-acid sites and of the surface concentration of Brønsted-acid sites, whereas the strength of Brønsted- and the surface concentration of Lewis-acid sites are not significantly affected. For constant vanadium loading, the composition of the mixed support strongly influences the surface concentration of both kinds of acid sites, especially in the range 0–10 wt% Al_2O_3. © 1995 Academic Press, Inc.

INTRODUCTION

Binary oxides of TiO_2 with Al_2O_3 have been used as mixed supports or as catalysts for various reactions such as the hydrodesulfurization (1–3), the isomerization of 1-butene and the dehydration of 2-butanol (4), the photocatalytic hydrogenation of propene and the isomerization of *cis*-2-butene (5), and the selective catalytic reduction (SCR) of NO by NH_3 in the presence of excess O_2 (6–9). In addition these binary oxides have been used as improved SMSI supports with high surface area, thermal stability and mechanical strength for metal catalysts (10–13).

Concerning the SCR reaction (for SO_2-containing feeds), it has been reported that vanadia catalysts supported on mixed TiO_2–Al_2O_3 carriers exhibit better catalytic properties as compared to conventional V_2O_5/TiO_2 catalysts, namely, a higher resistance toward deactivation by SO_2 and superior mechanical strength and thermal stability (6–9).

These studies of the V_2O_5/TiO_2–Al_2O_3 catalysts up to now were mainly focused on the influence of the preparation method and composition on the dispersion of TiO_2 on the alumina surface, the catalytic activity, and selectivity for the SCR reaction, as well as on the exhibited resistance toward deactivation by SO_2. It is well known, however, that the acidity of SCR catalysts plays an important role on their catalytic behavior since the progress of the reaction of NO with NH_3 requires activation of the latter on the acid centers of the catalyst. NH_4^+, NH_2, and NH_3 adsorbed forms have been considered as activated species participating in the reaction (14–17). To our knowledge the acidity of the V_2O_5/TiO_2–Al_2O_3 catalysts has not been studied yet.

In this work we study (using FTIR of chemisorbed NH_3) the influence of the composition on the acidity of the V_2O_5/TiO_2–Al_2O_3 catalysts. Two series of catalysts were prepared. In the first a constant loading of vanadium was deposited on a series of mixed TiO_2–Al_2O_3 with various compositions, whereas in the second series of catalysts various amounts of vanadium were supported on one TiO_2–Al_2O_3 support. The structure of these catalysts and the oxidation states of supported vanadium species were studied using XRD, IR, and XPS.

EXPERIMENTAL

Preparation of Catalysts

Pure TiO_2 (anatase) and five mixed TiO_2–Al_2O_3 supports (with alumina contents of 0, 2, 5, 10, 20, and 82 wt%) prepared by the method of gel-supported precipitation (18), a variant of the sol–gel method, were provided by Temav S.p.a. (Medicina, Italy). The same content of V_2O_5 (7.5 wt%) was deposited on these supports by wet impregnation with aqueous solution of vanadium oxalate. After

---

[1] To whom correspondence should be addressed at present address: Institute of Chemical Engineering and High Temperature Chemical Processes, University of Patras, P.O. Box 1414, 26500 Patras, Greece.

0021-9517/95 $12.00

TABLE 1

Specific Surface Areas (S_{BET}) of the TiO_2–Al_2O_3 Mixed Supports and the V_2O_5/TiO_2–Al_2O_3 Catalysts

Sample	S_{BET} (m^2/g)	Sample	S_{BET} (m^2/g)	Sample	S_{BET} (m^2/g)
TA2	85	TA2V7.5	53	TA10V4.5	160
TA5	152	TA5V7.5	110	TA10V6	164
TA10	199	TA10V7.5	132	TA10V7.5	132
TA20	290	TA20V7.5	171	TA10V9	118
TA82	280	TA82V7.5	249	TA10V10.5	108

stirring for 1 h, the solvent was removed with a rotary evaporator. The solids were then dried at 383 K for 5 h and calcined at 793 K for 16 h. Using the same procedure, a second series of catalysts was prepared by depositing various loadings of V_2O_5 (4.5, 6, 7.5, 9, and 10.5 wt%) on the TiO_2–Al_2O_3 10 wt% support.

We will denote by TA*x*, TA*x*V7.5, and TA10V*y* the supports and the two series of catalysts, respectively. The BET specific surface areas of these samples are reported in Table 1.

X-Ray Diffraction Analysis (XRD)

X-ray diffraction patterns were recorded on a Kristalloflex 805 (Siemens) diffractometer equipped with a Siemens D-500 detector using the Cu$K\alpha$ radiation.

X-Ray Photoelectron Spectroscopy (XPS)

The XPS analysis was performed at room temperature with a SSX-100 model 206 Surface Science Instruments (SSI) photoelectron spectrometer, interfaced to a Hewlett–Packard 9000/310 computer. The residual pressure in the spectrometer was in the range 1.3 to $6.5 \cdot 10^{-7}$ Pa. A monochromated Al anode (energy of the Al$K\alpha$ line 1486.6 eV), powered at 10 keV and 20 mA, was used for X-ray production. The binding energy scale of the spectrometer was calibrated with the Au $4f_{7/2}$ line (binding energy 83.98 eV). The analyzer energy and spot size were, respectively, 50 eV and 1.4 mm^2. These conditions give a full width at half maximum (FWHM) on Au $4f_{7/2}$ of 1 eV. The positive charge, developed on the samples due to the photoejection process, was compensated by a charge neutralizer (a flood gun) whose energy was adjusted at 6 eV (50 μA). The binding energies were calculated with respect to the C 1*s* peak ($\underline{C}$—C, $\underline{C}$—H) set at 284.6 eV. The intensities were estimated by calculating the integral of each peak after subtraction of the "S-shaped" background (19). Atomic concentration ratios were calculated by correcting the intensity ratios with the theoretical sensitivity factors based on Scoffield cross sections (20). The transmission function of the spectrometer was assumed to be independent of the kinetic energy (E_K) and electron mean free paths (IMFP) were taken to be proportional to $(E_K)^{0.7}$. Decomposition of peaks was done with the best fitting routine of the SSI instrument.

IR Spectroscopy

The IR spectra of all samples were recorded by a IFS 88 Brucker Fourier transform spectrophotometer (resolution 2 cm^{-1}). The KBr disc method was used. In order to obtain the IR spectra of supported vanadium the spectra of the supports TA*x* were subtracted from the ones of the corresponding catalysts, TA*x*V7.5 or TA10V*y*, using the data station of the spectrophotometer.

IR Spectroscopy of Chemisorbed Ammonia

In order to study by IR the ammonia chemisorbed on our samples the above mentioned spectrophotometer (resolution 2 cm^{-1}) was connected to a conventional evacuation/gas-manipulation greaseless ramp and IR cell (NaCl windows). The powder samples (ca. 15 mg) were pressed into self-supporting disks of appropriate thickness. Before the adsorption experiment the wafer of the pure sample powder was activated by outgassing at 443 K for 40 min in the IR cell and then reoxidized by 13 kPa of O_2 at 453 K for 40 min. The FTIR spectrum of the sample was recorded and then NH_3 (67 kPa) was introduced into the IR cell remaining in contact with the surface of each sample for 20 min. FTIR spectra were taken after three subsequent desorptions at 298, 353, and 403 K for 20 min. The spectra of the adsorbed species remaining after each desorption step were obtained by subtracting the contribution of the activated pure sample. The measured band intensities were normalized for the specific surface areas of the samples (by dividing the measured intensity by the surface area of the analyzed specimen) and were expressed as intensity/m^2 of sample. The FTIR spectra were also normalized in that way and are presented as absorbanse/m^2 vs wavenumber plots. The intensity ratios (intensity of a band after desorption at 403 K)/(intensity of the same band after desorption at 298 K), I_{130}/I_{25}, were calculated and used as a measure of the strength of the site giving rise to this band (21).

RESULTS

XRD Analysis

XRD analysis showed the presence of TiO_2 anatase in all samples. No diffraction lines assignable to TiO_2 (rutile) or lines assignable to any other phase, such as intermediate or mixed compounds, were detected in any sample.

In the case of the TA*x*V7.5 catalysts, V_2O_5 crystallites were detected only for the TA0V7.5 and TA2V7.5 samples.

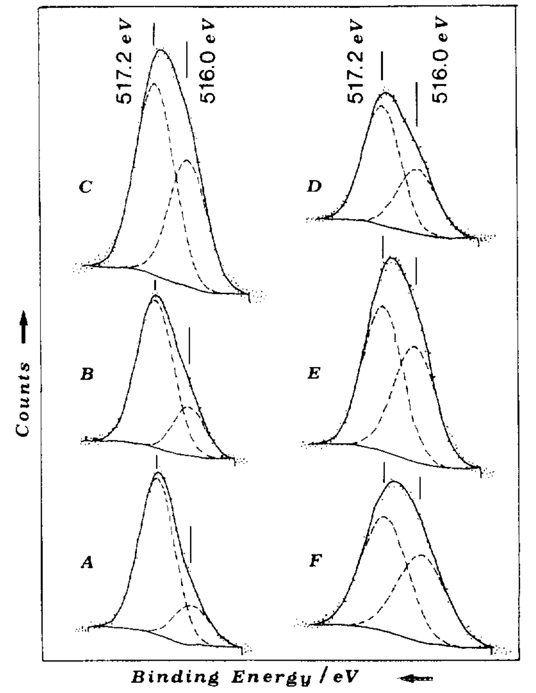

FIG. 1. Deconvoluted XPS spectra of the V $2p_{3/2}$ main photoelectron line of the TAxV7.5 catalysts: (A) x = 0, (B) x = 2, (C) x = 5, (D) x = 10, (E) x = 20, and (F) x = 82 wt% Al_2O_3. Binding energies are reported with an accuracy of ±0.1 eV.

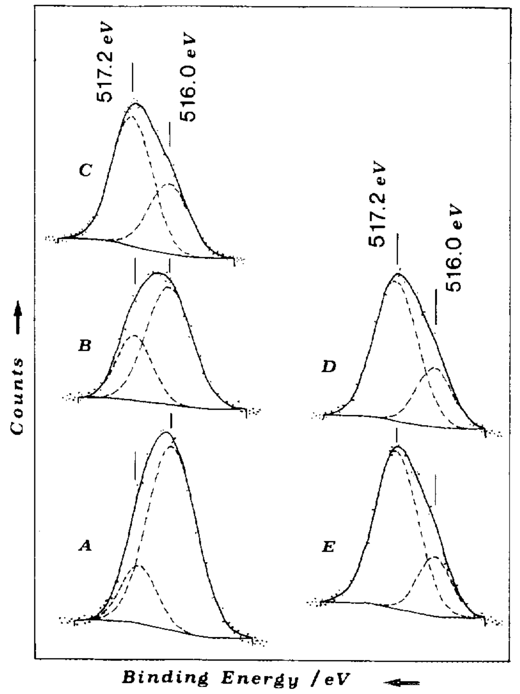

FIG. 2. Deconvoluted XPS spectra of the V $2p_{3/2}$ main photoelectron line of the TA10Vy catalysts: (A) y = 4.5, (B) y = 6, (C) y = 7.5, (D) y = 9, (E) y = 10.5 wt% V_2O_5. Binding energies are reported with an accuracy of ±0.1 eV.

No V_2O_5 crystallites were detected for all samples of the TA10Vy series.

XPS

For all samples studied the binding energy (BE) values of the Ti $2p_{3/2}$ and Al $2p$ photoelectrons were constant and equal to 458.4 ± 0.1 and 74.1 ± 0.1 eV, respectively. The Al $2p$ peak was slightly asymmetric for the samples containing the lowest amount of alumina (2 wt% Al_2O_3).

For both series of vanadium-containing samples, namely the TAxV7.5 and TA10Vy series, the profiles of the V $2p_{1/2}$ and V $2p_{3/2}$ lines were highly asymmetric suggesting the presence of two types of vanadium on the surface of the catalysts. The deconvolution of the V $2p$ XP spectra based on a Gaussian signal for the two types of vanadium led to a good fitting of the results (Fig. 1 and Fig. 2). The binding energies thus found (516.0 and 517.2 eV for the V $2p_{3/2}$ line) correspond to the values of V^{4+} in V_2O_4 and V^{5+} in V_2O_5, respectively (22–24).

The fraction of surface V^{4+} (expressed by the XPS atomic ratio $V^{4+}/(V^{4+} + V^{5+})$) on the TAxV7.5 samples is plotted vs the alumina content in Fig. 3. It can be seen that as the alumina content increases from 0 to 20 wt% Al_2O_3 the portion of surface V^{4+} continuously increases from ca.20 up to ca.50% of the total surface vanadium detected by XPS. Further increase of the alumina loading to 82 wt% does not significantly influence the amount of surface V^{4+}.

The variation of the $V^{4+}/(V^{4+} + V^{5+})$ XPS ratio of the TA10Vy samples with the vanadium loading is plotted in Fig. 4. The fraction of surface V^{IV} decreases rapidly as the vanadium loading increases from 4.5 to 7.5 wt% V_2O_5 and then decreases slightly for further increase of the vanadium content up to 10.5 wt%.

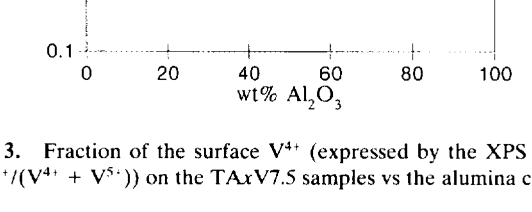

FIG. 3. Fraction of the surface V^{4+} (expressed by the XPS atomic ratio $V^{4+}/(V^{4+} + V^{5+})$) on the TAxV7.5 samples vs the alumina content.

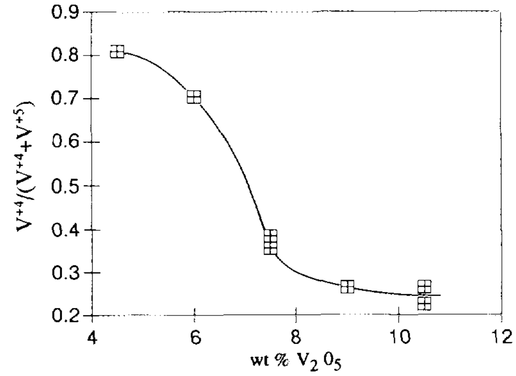

FIG. 4. Fraction of the surface V^{4+} (expressed by the XPS atomic ratio $V^{4+}/(V^{4+} + V^{5+})$) on the TA10Vy samples vs the vanadium content.

FTIR Spectra of Catalysts

The FTIR spectra of the TAxV7.5 catalysts, along with that of unsupported V_2O_5, are presented in Fig. 5.

Unsupported V_2O_5 shows essentially one peak at 1025 cm^{-1}, which has been assigned to the stretching vibrations of the short double bond $(V{=}O)^{3+}$ (25, 26). The spectrum of the TA0V7.5 catalyst is almost identical to that of unsupported V_2O_5; the only difference being a slight shift toward lower wavenumbers of the 1025 cm^{-1} peak appearing now at 1022 cm^{-1}.

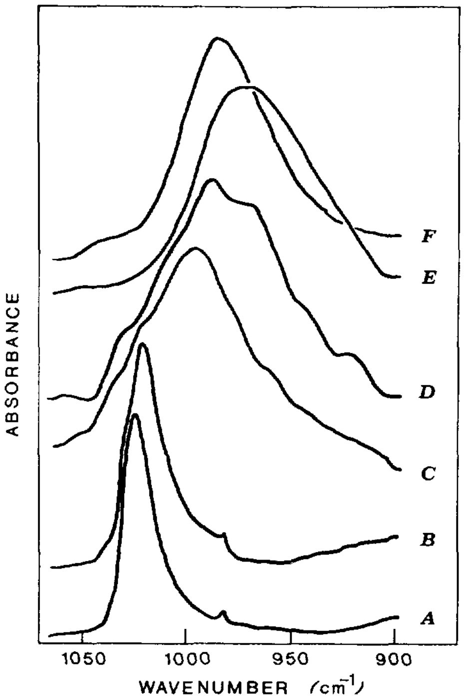

FIG. 5. FTIR spectra of the TAxV7.5 catalysts and of unsupported V_2O_5: (A) V_2O_5, (B) $x = 0$, (C) $x = 2$, (D) $x = 5$, (E) $x = 10$, and (F) $x = 20$ or 82 wt% Al_2O_3.

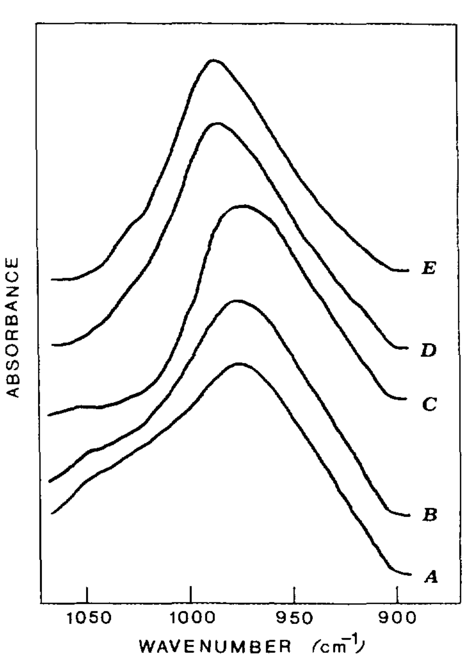

FIG. 6. FTIR spectra of the TA10Vy catalysts: (A) $y = 4.5$, (B) $y = 6$, (C) $y = 7.5$, (D) $y = 9$, and (E) $y = 10.5$ wt% V_2O_5.

The appearance of the IR spectrum changes dramatically in the case of the TA2V7.5 catalyst; it is now composed of a broad band centered at 997 cm^{-1} with weak broad shoulders at 1021 and 1030 cm^{-1}. As the Al_2O_3 content increases to 5 wt% (TA5V7.5) the IR spectrum becomes more complex. The broad band shifts toward lower wavenumbers and seems to present two maxima at 990 and 972 cm^{-1}. The shoulder at 1030 cm^{-1} is still present, but the one at 1021 cm^{-1} appears now at 1010 cm^{-1}. In the case of the TA10V7.5 sample the spectrum is dominated by a very broad absorbance band at 974 cm^{-1}; for higher Al_2O_3 contents (TA20V7.5 and TA82V7.5) this band becomes narrower and is centered at ca. 986 cm^{-1}.

The FTIR spectra of the TA10Vy catalysts are presented in Fig. 6. The spectrum of the TA10V4.5 sample consists of a very broad band centered at ca. 974 cm^{-1} and of a shoulder at 1048 cm^{-1}. As the vanadium loading increases to 7.5 wt% V_2O_5 (samples TA10V6 and TA10V7.5) the band at 974 cm^{-1} becomes narrower whereas the 1048 cm^{-1} shoulder progressively disappears. As the vanadium content increases further to 9.0 and 10.5 wt% the band shifts to 986 cm^{-1}. In addition, a shoulder at 1021 cm^{-1} appears for the maximum V_2O_5 content.

FTIR Spectroscopy of Chemisorbed Ammonia

The FTIR spectra of ammonia chemisorbed on the TAx supports, on the series of TAxV7.5, and on the series of the TA10Vy catalysts are presented in Fig. 7, Fig. 8, and Fig. 9, respectively. In order to facilitate the presentation

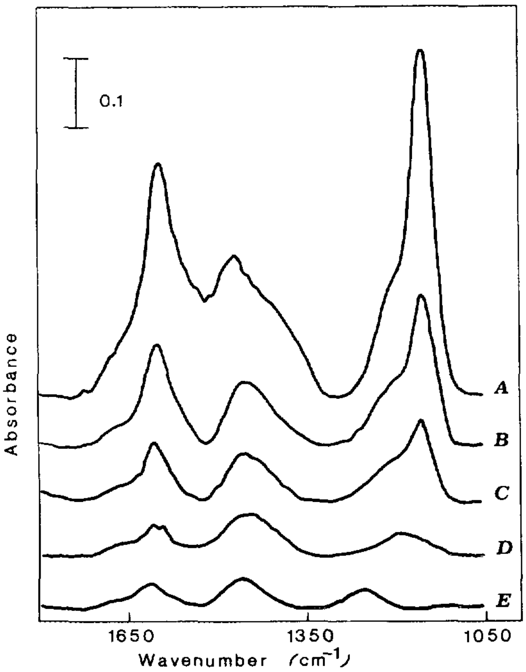

FIG. 7. FTIR spectra of NH_3 chemisorbed on the TA*x* mixed supports, after desorption at 25°C: (A) $x = 2$, (B) $x = 5$, (C) $x = 10$, (D) $x = 20$, and (E) $x = 82$ wt% Al_2O_3. Absorbance is expressed as absorbance (a.u.) per m^2 of sample.

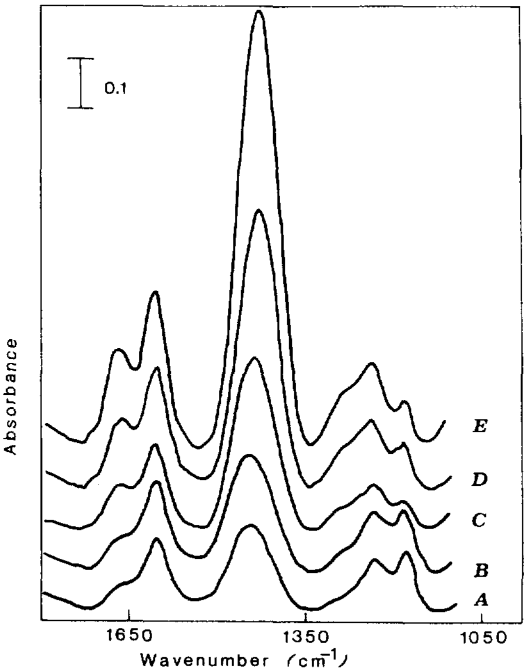

FIG. 9. FTIR spectra of NH_3 chemisorbed on the TA10V*y* catalysts, after desorption at 25°C: (A) $y = 4.5$, (B) $y = 6$, (C) $y = 7.5$, (D) $y = 9$, and (E) $y = 10.5$ wt% V_2O_5. Absorbance is expressed as absorbance (a.u.) per m^2 of sample.

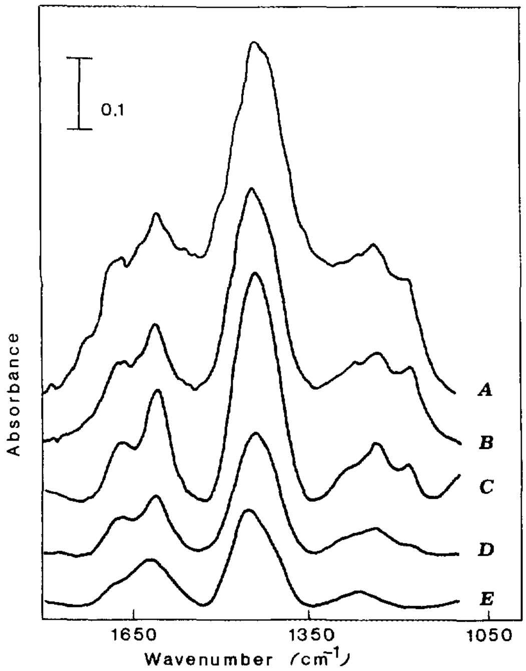

FIG. 8. FTIR spectra of NH_3 chemisorbed on the TA*x*V7.5 catalysts, after desorption at 25°C: (A) $x = 2$, (B) $x = 5$, (C) $x = 10$, (D) $x = 20$, and (E) $x = 82$ wt% Al_2O_3. Absorbance is expressed as absorbance (a.u.) per m^2 of sample.

of the results we will divide these spectra into five regions and discuss each one separately. For the same reason, a first attribution of the observed bands will be done in this section.

Region 1600–1620 cm^{-1}. For all samples studied one well defined absorbance band is observed in this region. IR studies of ammonia chemisorbed on titania have shown the presence of a band in the region 1600–1610 cm^{-1}; it has been attributed to the asymmetric deformation (δ_{as} NH_3) of ammonia coordinatively bonded to Lewis-acid sites of titania (27–29). In the case of alumina a band due to the asymmetric deformation of NH_3 coordinatively bonded to Lewis sites also appears in this region, but at higher wavenumbers, namely at 1610–1620 cm^{-1} (30, 31). Thus, the band appearing for our samples in the region 1600–1620 cm^{-1} is due to Lewis-acid sites present on the surface of both titania and alumina.

For all samples studied, the desorption temperature had no influence on the position of this band. In contrast, its position was found to depend on the content of both alumina and vanadium. Indeed, for the TA*x* supports it is shifted from 1601 to 1615 cm^{-1} as the alumina content increases. The same trend is observed in the case of the TA*x*V7.5 catalysts; the band shifts from 1603 to 1618 cm^{-1} as the alumina content increases up to 82 wt%. In the case of the TA*x*V7.5 catalysts, this band is always slightly shifted

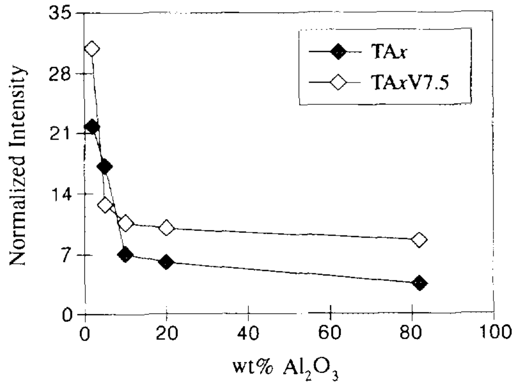

FIG. 10. Variation of the normalized intensity of the 1600 cm^{-1} absorbance band (expressed as intensity per m^2 of sample) with the alumina content for the TAx supports and the TAxV7.5 catalysts.

toward a higher frequency than that of the corresponding TAx supports. In addition, a slight shift toward higher frequency (from 1603 to 1606 cm^{-1}) with the increase of the vanadium content is observed in the case of the TA10Vy catalysts.

The intensity of this band is markedly influenced by the alumina content, and, to a lesser extent, by the vanadium content. The variation of the intensity with the alumina content for the TAx supports is presented in Fig. 10. As the alumina content increases to 10 wt% an important decrease of the intensity is observed, whereas a further increase of the alumina content brings about only a very slight decrease. The same trend is observed for the $TA_xV7.5$ catalysts (Fig. 10). Concerning the influence of vanadium on the intensity, an inspection of Fig. 10 shows that its deposition on the TAx supports generally provokes a slight increase of this intensity. In addition, we found that the intensity of this band slightly increases with the vanadium loading in the series of the TA10Vy catalysts. However, as compared to the changes provoked to the intensity of the 1600–1620 cm^{-1} band by the alumina content, those due to the vanadium loading are rather small.

In all cases, the intensity ratio I_{130}/I_{25} of this band is not influenced by the alumina content; its value is 0.7–0.9 for the TAx supports and 0.8–1.0 for the TAxV7.5 catalysts. However, the presence of vanadium was found to influence this ratio; its value for a catalyst was always slightly higher than that of the corresponding support. In addition, a slight increase of this ratio with the vanadium content is observed in the case of the TA10Vy catalysts; it continuously increases from 0.7 for $y = 0$ to 0.9 for $y = 10.5$ wt% V_2O_5.

Region 1160–1240 cm^{-1}. For all samples containing up to 20 wt% Al_2O_3 two bands are observed in this region. Both bands disappear in the samples containing the maximum amount of alumina (82 wt%). IR studies of ammonia chemisorbed on titania have reported the presence of two bands in this region. The first appears, depending on the pretreatment used, at 1155–1180 cm^{-1}, whereas the second one appears in the form of a shoulder around 1200–1225 cm^{-1} (28, 29, 32). They have been attributed to the symmetric deformation of ammonia (δ_sNH_3) coordinatively bonded to two different types of Lewis sites on the surface of titania (32). These two distinct types of Lewis-acid sites correspond to surface Ti^{4+} ions in different stereochemical environments (33). According to Primet *et al.* (32) the first type of acid sites (the stronger one, giving rise to the 1200–1225 cm^{-1} band) is created by the removal of isolated OH groups, whereas the second (weaker) type is due to the removal of molecular water. Since, for pure alumina, no band appears in this region (31), the two bands appearing in the case of our samples are due to the two distinct Lewis sites of titania.

For all samples studied both bands shift (for about 10–15 cm^{-1}) toward higher frequency as the desorption temperature increases. In the case of the TAx supports the first band appears at 1160 cm^{-1} and the second one appears as a shoulder around 1200 cm^{-1}, whereas for the TAxV7.5 catalysts both bands appear at higher wavenumbers (at 1185 and 1235 cm^{-1}, respectively). For both series of samples the position of these bands as well as their I_{130}/I_{25} ratios were found to be independent of the alumina content. The variation of the intensity of these two bands with the alumina content, for the TAx supports and the TAxV7.5 catalysts, is plotted in Fig. 11. It is seen that, for both series of samples, the intensity of the bands decreases as the alumina content increases; this decrease is more pronounced for the 1160 cm^{-1} band in the case of the supports. One may also observe that the addition of vanadium strongly suppresses the intensity of the low wavenumber band, while it leaves unaffected the intensity of the high wavenumber one.

For the TA10Vy catalysts the bands appear at around

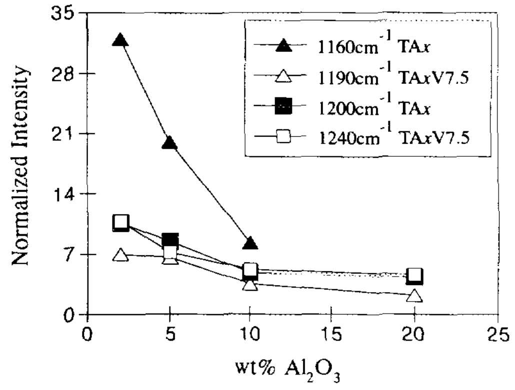

FIG. 11. Variation of the normalized intensity of the 1160, 1190, 1200, and 1240 cm^{-1} absorbance bands (expressed as intensity per m^2 of sample) with the alumina content for the TAx supports and the TAxV7.5 catalysts.

1180 and 1235 cm^{-1}; these values are higher than those of the corresponding TA10 support (1163 and 1200 cm^{-1}, respectively). In addition, both bands shift toward higher frequency (from 1163 to 1185 cm^{-1} and from 1200 to 1240 cm^{-1}) as the vanadium content increases from 0 to 10.5 wt% V_2O_5. The intensity of the low wavenumber band decreases continuously as the vanadium loading increases, contrary to the high wavenumber one whose intensity was found to be constant, independent of the vanadium loading. Finally, vanadium was found to influence the I_{130}/I_{25} ratios of both bands; they slightly increase with the V_2O_5 content. In addition, these ratios had higher values in the case of the TA*x*V7.5 catalysts than in the corresponding TA*x* supports.

Region 1250–1290 cm^{-1}. A band at 1260 cm^{-1} appears in the IR spectrum of the TA82 support; it appears as a shoulder for the TA20 and not at all for lower alumina contents. This band is due to the symmetric deformation of ammonia (δ_sNH_3) coordinatively bonded to one type of the Lewis-acid sites of alumina (14, 27, 31, 34).

In the case of the TA*x*V7.5 catalysts two absorbance bands are generally observed in this region. One appears only for the TA82V7.5 catalyst at 1265 cm^{-1}; thus it is somehow shifted as compared to that of the corresponding TA82 support. The other band appears in the form of a shoulder around 1290 cm^{-1} for the catalysts containing 5 to 20 wt% Al_2O_3, although it is quite possible that it also exists for the TA82V7.5 catalyst but is masked by the more intense 1265 cm^{-1} band. A shoulder around 1290 cm^{-1} has been reported in several studies of V_2O_5/Al_2O_3 catalysts (21, 35). Since it has never been observed for V_2O_5/TiO_2 catalysts (26, 28), we attribute the 1290 cm^{-1} shoulder appearing in our TA*x*V7.5 samples to the presence of Lewis sites associating both alumina and vanadium. Finally in the case of the TA10V*y* catalysts only the shoulder around 1290 cm^{-1} is observed.

Region 1430–1470 cm^{-1}. For all samples studied one absorbance band is observed in this region; it is due to the asymmetric deformation of ammonium ions chemisorbed on Brønsted sites (26, 27, 36, 37).

This band appears at 1455 cm^{-1} for the TA*x* supports with the exception of TA2, for which it appears as an ill-shaped band around 1470 cm^{-1}. The desorption temperature had no influence on the position of this band. The variation of the intensity with the alumina content is presented in Fig. 12. As the alumina content increases from 2 to 20 wt% an important decrease of the intensity is observed, whereas a further increase of alumina to 82 wt% leaves the intensity unaffected. The I_{130}/I_{25} ratios for the alumina-poor supports (TA2 and TA5) were higher (0.7 ± 0.1) than those of the alumina rich ones (0.4 ± 0.1). These ratios are in all cases lower than those of the bands due to Lewis acidity.

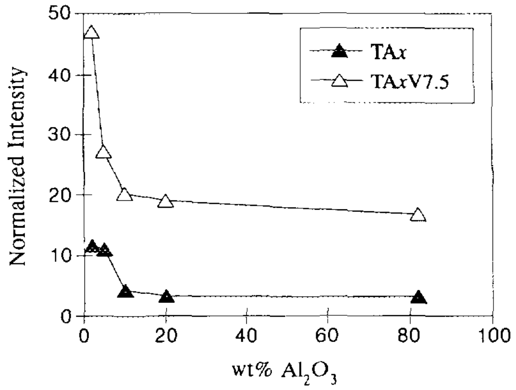

FIG. 12. Variation of the normalized intensity of the 1450 cm^{-1} absorbance band (expressed as intensity per m^2 of sample) with the alumina content for the TA*x* supports and the TA*x*V7.5 catalysts.

In the case of the TA*x*V7.5 catalysts this band appears at around 1435 cm^{-1}. As compared to the corresponding supports it is now shifted toward lower wavenumbers and is much more intense. As the alumina content increases (from 2 to 82 wt%) the band shifts to higher wavenumbers (from 1430 to 1445 cm^{-1}). As seen from Fig. 12 the intensity of the band strongly diminishes as the alumina content increases up to 10 wt% and then it remains practically constant for a further increase of the Al_2O_3 content to 82 wt%. An inspection of the same figure (Fig. 12) clearly shows that the deposition of a fixed amount of vanadium on the TA*x* supports provokes an important increase on the intensity of this band.

In the case of the TA10V*y* catalysts this band shifts progressively from 1453 to 1430 cm^{-1} as the V_2O_5 loading increases from 0 to 10.5 wr%. The variation of the intensity with the vanadium content is plotted in Fig. 13; a continuous increase with the V_2O_5 loading is observed. The ratio I_{130}/I_{25} remains practically constant (0.36 ± 0.06) for vana-

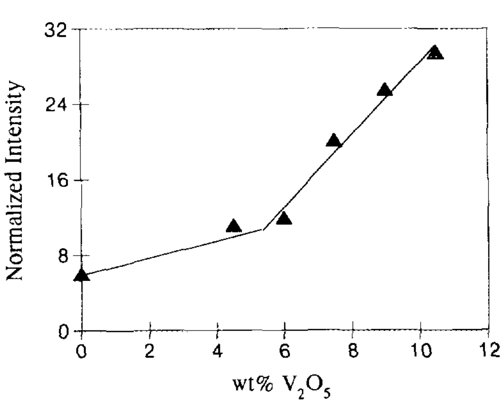

FIG. 13. Variation of the normalized intensity of the 1450 cm^{-1} absorbance band (expressed as intensity per m^2 of sample) with the vanadium loading for the TA10V*y* catalyst.

dium loadings in the range 0 to 9 wt%; it becomes considerably higher (0.62) for the maximum vanadium loading (10.5 wt% V_2O_5).

For both series of catalysts (TAxV7.5 and TA10Vy) a slight shift of this band toward lower frequencies with an increase of the desorption temperature was observed. As it was the case for the TAx supports, the I_{130}/I_{25} ratios always had lower values than those of bands due to Lewis acidity.

Region 1660–1680 cm^{-1}. For the TAx supports a small shoulder around 1660 cm^{-1} appears when the desorption temperature is 25°C; it generally disappears for higher temperatures. This shoulder becomes more important in the case of the TAxV7.5 catalysts, whereas its intensity was found to increase with the vanadium loading in the TA10Vy series. Its position was independent of the desorption temperature as well as of the content of both alumina and vanadium.

Absorbance in this region is due to the symmetric deformation of ammonium ions ($\delta_s NH_4^+$) (37, 38). Although no band in this region has been reported for unsupported V_2O_5 (26, 27, 39), one has been observed for the V_2O_5/TiO_2 and V_2O_5/Al_2O_3 catalysts (28, 31, 38). Taking into consideration that this band is visible for the TAx supports and becomes more important when vanadium is present (TAxV7.5), as well as the fact that its intensity increases with the vanadium loading (TA10Vy), we attribute this band to the presence of Brønsted sites on the surface of both supported vanadium and uncovered support.

DISCUSSION

Structure of V_2O_5/TiO_2–Al_2O_3 Catalysts

Bulk V_2O_5 is present in the TA0V7.5 sample as evidenced by both XRD analysis and its IR spectrum which was almost identical to that of bulk V_2O_5.

The presence of only 2 wt% Al_2O_3 on the support was found to induce important changes on the structure of supported vanadium. The XRD pattern of the TA2V7.5 sample shows that now only a part of supported vanadium is in the form of crystalline V_2O_5. This is also corroborated by the IR spectrum; only a shoulder at 1021 cm^{-1} (characteristic of V=O in bulk V_2O_5) is visible for this catalyst. The remaining part of vanadium is transformed to an XRD amorphous phase characterized by the IR band centered at 997 cm^{-1}. This shifting of the stretching vibration of the $(V{=}O)^{+3}$ double bond to lower frequencies indicates a weakening of this bond. Two effects may contribute to the weakening of the V=O bond. The first is a structural transformation. According to Centi *et al.* (22), this may be due to a change from the highly distorted pseudopyramidal coordination of vanadium in the V_2O_5 to nearly octahedral coordination. This is consistent with the observed loss of crystallinity and the formation of an amorphous supported phase (40). The second effect is an electronic one. The weakening of the double bond may also be due to the presence of neighboring V^{4+} ions (22, 25, 41, 42), which were detected by XPS on the surface of our samples.

No crystalline V_2O_5 was detected in the TAxV7.5 samples with alumina content higher than 2 wt%.

As the Al_2O_3 content increases to 10 wt% the broad IR band gradually shifts from 997 to 974 cm^{-1}. Roozeboom *et al.* (43) studied the vanadium species supported on various carriers by Raman spectroscopy; they concluded that the 970 cm^{-1} band is due to surface vanadate species present as a two-dimensional monolayer. According to Griffith and Lensniak (44) the band at 950–970 cm^{-1}, observed with polyvanadate ions containing ca. 10 vanadium atoms, originates from their distorted configuration.

The IR band for the samples with the higher alumina loadings (TA20V7.5 and TA82V7.5) appears at 986 cm^{-1}. Miyata *et al.* (42) have attributed this band also to the presence of an amorphous two-dimensional vanadium oxide phase; they have observed this band for both V_2O_5/TiO_2 and V_2O_5/Al_2O_3 systems with low vanadium contents.

We may thus conclude that adding alumina on the titania support, while keeping constant the loading of vanadium, provokes a drastic decrease of the V_2O_5 crystallinity. For alumina contents higher than 2 wt% Al_2O_3 supported vanadium is in the form of an amorphous two-dimensional phase. Recent studies of V_2O_5/TiO_2 and V_2O_5/Al_2O_3 catalysts, based mostly on Raman (LRS) and ^{51}V NMR spectroscopies (45, 46), have shown that this amorphous dispersed phase is composed of both monomeric vanadyl and polymeric vanadate species. The relative abundance of these two structures varies with the surface concentration of vanadia. At low surface concentrations the monomeric vanadyls predominate. As the surface concentration of vanadia increases polymeric vanadate species are formed at the expense of the monomeric vanadyls.

No bulk V_2O_5 could be detected by XRD for all the samples of the TA10Vy series. For vanadium loadings in the region 4.5 to 7.5 wt% V_2O_5 the FTIR spectra of the samples exhibit essentially one broad band at ca. 974 cm^{-1} indicating the presence of a two-dimensional amorphous vanadium phase. For high vanadium loadings (samples TA10V9 and TA10V10.5) one can observe, besides a slight shift of the main IR band to 986 cm^{-1}, the progressive appearance of a small shoulder at 1021 cm^{-1}. Thus for these loadings a very small portion of supported vanadium forms crystalline V_2O_5.

Oxidation State of Vanadium Species

Concerning the oxidation state of supported vanadium, our XPS results showed the presence of both V^{4+} and V^{5+} supported species on the surface of the V_2O_5/TiO_2–Al_2O_3 catalysts and, furthermore, that the ratio V^{4+}/V^{5+} strongly depends on the composition. It is known from the literature (mostly from studies using XPS, ESR, and chemical titrations) that V^{4+} species are stabilized on both V_2O_5/TiO_2 and V_2O_5/Al_2O_3 systems (23, 24, 31, 47–52). Although the stabilization of V^{4+} species, strongly interacting with the carrier, on supported vanadia catalysts and the localization of these species on the surface of the support are well shown in the literature, the precise mechanism of their formation during calcination under aerobic conditions is not yet clear.

As shown in Fig. 4 the ratio V^{4+}/V^{5+} decreases as the vanadium loading increases in the TA10V*y* series. A similar behavior has been reported in the case of V_2O_5/TiO_2 catalysts (24, 52). This is most probably due to the fact that as the loading of vanadium increases the ratio (vanadium strongly interacting with the support)/(total vanadium) decreases.

What seems to be of considerable interest is the behavior of the TA*x*V7.5 series. As seen from Fig. 3 the ratio V^{4+}/V^{5+} can be controlled by the composition of the support while keeping constant the total loading of vanadium. The possibility to tune the ratio V^{4+}/V^{5+} to a desired value by suitable selection of the support composition may prove very useful for those vanadia-catalyzed reactions where the relative distribution of V^{4+} and V^{5+} species influences the activity and/or the selectivity. The selective oxidation of *o*-xylene (50) and the selective catalytic reduction of NO with NH_3 in the presence of SO_2 (6, 8) are typical examples of such reactions.

Influence of the V_2O_5 Content on the Acidity

It is well established that V_2O_5 exhibits essentially Brønsted acidity (14, 26, 27). In the case of our catalysts, the deposition of V_2O_5 on the TiO_2–Al_2O_3 mixed supports influences the position of absorbance bands due to the symmetric deformation of ammonia ($\delta_s NH_3$) characteristic of Lewis acidity. This mode of vibration gives IR bands appearing in a large region; namely, from 932–938 cm^{-1} for gaseous NH_3 to 1300 cm^{-1} for ammonia coordinatively bonded to strong acid sites. As the strength of the acid site increases the band is shifted toward higher frequencies (35, 53, 54). The bands due to the two types of Lewis acid sites on TiO_2, appearing at 1160 and 1200 cm^{-1} in the case of the support, are shifted to around 1190 and 1240 cm^{-1}, respectively, after the deposition of V_2O_5. The same effect is observed in the case of TA10V*y* catalysts; as the V_2O_5 content increases these two bands are shifted toward higher frequencies. The influence of V_2O_5 on the position of the band around 1260 cm^{-1} (characteristic of ammonia bonded to Lewis acid sites on the alumina surface) is not so evident since, with the exception of samples containing the maximum amount of alumina, it appears as a shoulder whose position cannot be accurately determined. In the TA82V7.5, however, this band is shifted toward a higher wavenumber than the corresponding band of the TA82 support. In addition the catalysts TA*x*V7.5 and TA10V*y* exhibit a shoulder around 1290 cm^{-1} which does not appear in the case of the supports. Thus, the addition of V_2O_5 provokes the shifting of the bands due to the $\delta_s NH_3$ mode of vibration toward higher frequencies. This clearly proves that vanadium increases the strength of the Lewis-acid sites.

This conclusion is further corroborated by the evolution of the intensity ratios I_{130}/I_{25} of the band around 1600 cm^{-1} (characteristic of Lewis sites on titania and alumina) with the V_2O_5 content in the TA10V*y* catalysts. The observed continuous increase of this ratio with the vanadium content indicates that an increasing proportion of ammonia molecules remain bonded on the surface after desorption at higher temperature. Thus, an increasing proportion of Lewis-acid sites become stronger as the V_2O_5 content increases. An additional confirmation comes from the comparison of the ratios I_{130}/I_{25} for the 1600 cm^{-1} band of the catalysts TA*x*V7.5 with those of the corresponding supports TA*x*. Regardless of the alumina content the ratio of the catalysts is always higher than that of the corresponding supports. The same behavior is observed with the I_{130}/I_{25} ratios of the other bands characteristic of Lewis acidity.

Both types of results (namely, the shifting and the intensity ratios of bands corresponding to Lewis acidity) clearly demonstrate that, although vanadium oxide has by itself essentially protonic acidity, its deposition on the TiO_2–Al_2O_3 supports provokes an increase of the electron acceptability of the surface, thus inducing the formation of stronger Lewis-acid sites than those existing on the surface of the supports.

The stronger Lewis acidity of the catalysts as compared to that of the corresponding supports may be the result of two mechanisms: Vanadium might either influence a vicinal Lewis site, located on the uncovered support surface, and render it a stronger acid site, or it might directly participate, through its interaction with the components of the support, in the creation of new strong Lewis-acid sites. The evolution of the intensities of the bands (due to the presence of Lewis sites), as well as the appearance of new bands, with the V_2O_5 content will be useful in order to clarify this point.

In the case of the TA10V*y* catalysts, the intensity of the band around 1600 cm^{-1} continuously increases with the vanadium content. In addition this intensity is higher in the case of the TA*x*V7.5 catalysts than that of the corresponding supports TA*x* (Fig. 10). Thus, the band around 1600 cm^{-1} cannot be attributed exclusively to Lewis sites on the uncovered support; indeed, if this was the case then the intensity should diminish with an increase of the vanadium loading. It is probable that this increase of the Lewis acidity is due to the creation of new sites resulting from the interaction between supported phase and support. The first to propose this hypothesis were Sobalik *et al.* (16, 55) who also observed for V_2O_5/Al_2O_3 catalysts an increase of the intensity of the 1600 cm^{-1} band with the vanadium content. They attributed this phenomenon to the creation of new Lewis sites from the interaction of vanadium with alumina. Dines *et al.* (38) observed the same phenomenon in the case of V_2O_5/TiO_2 catalysts. They proposed that the Lewis acid sites on the surface of these catalysts are due at least in part to coordinatively unsaturated vanadium ions on the surface as well as to exposed TiO_2. It is, thus, reasonable to assume, for the TA*x*V7.5 and TA10V*y* catalysts, that the band around 1600–1620 cm^{-1} is due to both the Lewis sites of the mixed support (which remains uncovered) and to the new strong Lewis sites resulting from the interaction V–Al and V–Ti.

The band around 1290 cm^{-1}, appearing for the TA*x*V7.5 and TA10V*y* catalysts but not for the TA*x* supports, is (because of its high wavenumber value) characteristic of very strong Lewis-acid sites. Bands in this region have been reported only for V_2O_5/Al_2O_3 catalysts (21, 35, 55). In addition, the position of this band in the catalysts is substantially higher than that of the alumina support (around 1260 cm^{-1}). Sobalik *et al.* (16) have demonstrated that vanadium ions shift this band toward higher frequencies. They also found that as the oxidation state of vanadium decreases to +4, an increasing proportion of ammonia molecules remains chemisorbed onto these Lewis sites after desorption treatment at high temperature. This strongly suggests the participation of the V^{4+} ions, detected in our sample by XPS, in the creation of new Lewis-acid sites. Based on these facts we attribute the band at 1290 cm^{-1} to the new strong Lewis sites formed by the strong interaction of the low-valence vanadium ions with the alumina component of the mixed TiO_2–Al_2O_3 support.

The band appearing for the TA*x*V75. and TA10V*y* catalysts at 1240 cm^{-1} has only been observed in the case of V_2O_5/TiO_2 catalysts (26, 28, 29). On pure TiO_2 this band appears at a lower frequency, namely, at 1200–1225 cm^{-1} (32). Busca (28) attributed this band to Lewis sites formed by coordinatively unsaturated vanadyl groups isolated on the surface of titania. Thus, here again, the observed increase of the strength of Lewis acidity of the catalysts, as compared to that of the corresponding supports, is due to the formation of new stronger acid sites.

Finally, the intensity of the band around 1190 cm^{-1} decreases with the V_2O_5 content (series TA10V*y*). This clearly shows that this band is only due to NH_3 chemisorption on Lewis sites of the uncovered titania surface in the support. Busca (28) arrived to the same conclusion by comparing spectra obtained after adsorption of NH_3 with those obtained after adsorption of CO on V_2O_5/TiO_2 catalysts. They reported that the intensity of both the $\delta_s NH_3$ band around 1190 cm^{-1} and the band due to CO chemisorbed on uncovered TiO_2 diminish as the vanadium content increases. Thus, concerning these Lewis sites on titania, although the direct participation of vanadium is excluded, its addition contributes to the strengthening of these sites probably by some electron withdrawal effect.

We may, thus, conclude that the observed stronger Lewis acidity of the catalysts, as compared to that of the corresponding supports, is the result of the application of both mechanisms. New stronger Lewis sites are formed with the direct participation of vanadium, and preexisting Lewis sites on the uncovered support are strengthened due to the influence exerted by vicinal supported vanadium.

The influence of vanadium on the total concentration of Lewis-acid sites is difficult to ascertain. The intensity of the 1600 cm^{-1} band increases with the vanadium content in the TA10V*y* series. In addition the intensity of this band for the TA*x*V7.5 catalysts is generally higher than that of the corresponding TA*x* supports. Thus, the presence of vanadium induces the increase of the concentration of the Lewis sites responsible for the appearance of this band. However, as we have already seen, the evolution of the intensity of the other bands, characteristic of Lewis acidity, with the vanadium content does not follow the same trend; the intensity of the 1190 cm^{-1} band decreases, that of the 1240 cm^{-1} band remains practically constant, whereas that of the 1290 cm^{-1} band cannot be accurately determined since it appears as a shoulder. However, since the observed changes in the intensities are rather small, the influence of vanadium on the total concentration of Lewis sites can practically be considered as negligible.

The evaluation of the vanadium influence on the strength of the Brønsted sites will be based on the intensity ratios I_{130}/I_{25} of the band appearing in the region 1430–1470 cm^{-1} characteristic of protonic acidity. For the series of catalysts TA10V*y* this ratio remains practically constant for a loading up to 9 wt% V_2O_5; it increases for a further increase of the vanadium content. Thus, the strength of Brønsted acid sites is not modified (increased) for vanadium loadings lower than 9 wt%. However the observed changes in the I_{130}/I_{25} ratios are rather small. So, it seems that, contrary to the influence of vanadium on the strength of Lewis sites, the observed strengthening of Brønsted sites is not so important. It should also be noted that for all samples studied the ratios I_{130}/I_{25} of bands due to Brønsted sites are always lower than those of bands due to the existence of Lewis sites; this suggests that the strength of Brønsted sites is inferior to that of Lewis-acid sites.

The concentration of Brønsted-acid sites, in contrast, to that of Lewis sites, is markedly influenced by the vanadium loading. Indeed, the intensity of the 1430 cm^{-1} band strongly increases as the V_2O_5 loading increases in the TA10V*y* catalysts (Fig. 13). The same trend is observed for the other band (1660 cm^{-1}) characteristic of Brønsted acidity. In addition, the intensity of this band is much higher in the case of the TA*x*V7.5 catalysts as compared to that of the corresponding TA*x* supports (Fig. 12). These results clearly demonstrate that vanadium greatly enhances the total surface concentration of Brønsted acid sites of the V_2O_5/TiO_2–Al_2O_3 catalysts.

Influence of the Al_2O_3 Content on the Acidity

No significant influence of the alumina content on the strength of acid sites (Lewis and Brønsted) was observed for both the TA*x* supports and the series of TA*x*V7.5 catalysts. In contrast, the surface concentration of both kinds of acid sites is highly influenced by the alumina content. Indeed the intensities of the IR bands characteristic of both Lewis and Brønsted acidity greatly decrease with the increase of the alumina content up to 10 wt% and then they remain practically constant for a further increase of the alumina content up to 82 wt%. This behavior is common to both the TA*x* supports and the TA*x*V7.5 catalysts (Figs. 10, 11, and 12).

Finally, concerning the role of these mixed carriers, our results showed that the composition of the TiO_2–Al_2O_3 supports can regulate important properties of the V_2O_5/TiO_2–Al_2O_3 catalysts, such as the fraction of surface vanadium species stabilized as V^{4+}, or the surface concentration of both Lewis- and Brønsted-acid sites. This fact, along with their improved textural and mechanical properties, as compared to those of pure titania (6, 7), make their use attractive for supported vanadia catalysts. Their beneficial effect has already been reported for the SCR of NO by NH_3 in the presence of SO_2 (6–9) and their use seems to be promising also for other vanadia–catalyzed reactions, especially where a modification of acidic or redox properties is needed in order to improve the catalytic behavior.

CONCLUSIONS

The main objective of this work was to investigate the influence of the composition of the V_2O_5/TiO_2–Al_2O_3 catalysts on their acidity (based on the study of chemisorbed NH_3 by FTIR) and on the structural properties (as revealed by the results of the physicochemical characterization using XRD, XPS, and IR).

The most important conclusions are the following:

(i) Both V^{4+} and V^{5+} supported species were detected on the surface of the V_2O_5/TiO_2–Al_2O_3 catalysts. The ratio V^{4+}/V^{5+} depends on the vanadium content, whereas for constant vanadium loading it can be regulated by the composition of the mixed TiO_2–Al_2O_3 support.

(ii) The deposition of vanadium on the mixed TiO_2–Al_2O_3 supports increases the strength of the Lewis-acid sites. This was found to be due to both the formation of new stronger sites, with the direct participation of supported vanadium, and to the strengthening of preexisting Lewis sites on the uncovered support from vicinal supported vanadium species. The strength of Brønsted sites was found to slightly increase for vanadium loadings higher than 9 wt% V_2O_5.

(iii) The surface concentration of Brønsted-acid sites on the V_2O_5/TiO_2–Al_2O_3 catalysts is greatly enhanced as the loading of vanadium increases. In contrast, the surface concentration of Lewis-acid sites is not significantly affected by the deposition of vanadium.

(iv) For constant vanadium loading, the surface density of both kinds of acid sites is greatly influenced by the composition of the mixed TiO_2–Al_2O_3 support, especially in the composition range of 0 to 10 wt% Al_2O_3. The strength of both Lewis- and Brønsted-acid sites was found to be practically independent of the alumina content in the composition range studied.

REFERENCES

1. Zhaobin, W., Qin, X., Xiexian, G., Grange, P., and Delmon, B., *Appl. Catal.* **75,** 179 (1991).
2. Zhaobin, W., Qin, X., Xiexian, G., Sham, E., Grange, P., and Delmon, B., *Appl. Catal.* **63,** 305 (1990).
3. Spojakina, A., Damyanova, S., and Jiratova, K., *in* "Proceedings of the 12th Simposio Iberoamericano de Catalisis," p. 571.
4. Rodenas, E., Yamaguchi, T., Hattori, H., and Tanabe, K., *J. Catal.* **69,** 434 (1981).
5. Anpo, M., Kawamura, T., Kodama, S., Maruya, K., and Onishi, T., *J. Phys. Chem.* **92,** 438 (1988).
6. Clarebout, G., Ruwet, M., Matralis, H., and Grange, P., *Appl. Catal.* **76,** L9 (1991).
7. Centi, G., Militerno, S., Perathoner, S., Riva, A., and Brambilla, G., *J. Chem. Soc. Chem. Commun.,* 88 (1991).
8. Centi, G., Grange, P., Matralis, H., Ruwet, M., and Trifiro, F., *in* "Proceedings of 1st Japan–EC Joint Workshop on the Frontiers of Catalytic Science and Technology (JECAT'91)," p. 135. Tokyo, 1991.
9. Matralis, H., Fiasse, S., Castillo, R., Bastians, Ph., Ruwet, M., Grange, P., and Delmon, B., *Catal. Today* **17,** 141 (1993).
10. McVicker, G. B., and Ziemiak, J. J., *J. Catal.* **95,** 473 (1985).
11. Foger, K., and Anderson, J. R., *Appl.Catal.* **23,** 139 (1986).
12. Stranick, M. A., Houalla, M., and Hercules, D., *J. Catal.* **106,** 362 (1987).
13. Stranick, M. A., Houalla, M., and Hercules, D., *J. Catal.* **125,** 214 (1990).
14. Takagi, M., Kawai, T., Soma, M., and Tamaru, K., *J. Catal.* **50,** 441 (1977).
15. Markvart, M., and Pour, V., *in* "Proceedings of the 4th International Symposium on Heterogeneous Catalysis, Varna, 1979," Part 2, p. 93, 1979.
16. Sobalik, Z., Pour, V., Dosumov, K., and Sokalova, L., *React. Kinet. Catal. Lett.* **28,** 443 (1985).
17. Bosch, H., and Janssen, F., *Catal. Today* **2,** 369 (1988).
18. Brambilla, G., Centi, G., Perathoner, S., and Riva, A., *in* "Proceedings of the 2nd European Conference on Advanced Materials and Processes," p. 382. Institute of Metals Publications, London, 1991.
19. Shirley, D. A., *Phys. Rev.* **35,** 4709 (1972).
20. Scoffield, J. H., *J. Electron Spectrosc. Relat. Phenom.* **8,** 129 (1976).
21. Sobalik, Z., Pour, V., Cizek, M., Markvart, M., Nevskaya, O., and Sobolova, L., *in* "Proceedings, 6th International Symposium on Heterogeneous Catalysis, Sofia, 1987," p. 378.
22. Centi, G., Pinelli, D., Trifiro, F., Ghoussoub, D., Guelton, M., and Gengembre, L., *J. Catal.* **130,** 238 (1991).

23. Centi, G., Giamello, E., Pinelli, D., and Trifiro, F., *J. Catal.* **130,** 220 (1991).
24. Nogier, J. P., Jammul, N., and Delamar, M., *J. Electron. Spectrosc. Relat. Phenom.* **56,** 279 (1991).
25. Andersson, A., *J. Catal.* **76,** 144 (1982).
26. Inomata, M., Mori, K., Miyamoto, A., Ui, T., and Murakami, Y., *J. Phys. Chem.* **87,** 754 (1983).
27. Takagi, M., Kawai, T., Soma, M., Onishi, T., and Tamaru, K., *Can. J. Chem.* **58,** 2132 (1980).
28. Busca, G., *Langmuir* **2,** 577 (1986).
29. Rajudhyaksha, R., and Knozinger, H., *Appl. Catal.* **51,** 81 (1989).
30. Knozinger, H., *Adv. Catal.* **25,** 184 (1976).
31. Inomata, M., Mori, K., Miyamoto, A., and Murakami, Y., *J. Phys. Chem.* **87,** 761 (1983).
32. Primet, M., Pichat, P., and Mathieu, M., *J. Phys. Chem.* **75,** 1221 (1971).
33. Parfitt, G., Ramsbothen, J., and Rochester, C., *J. Chem. Soc. Faraday Trans. 1* **67,** 1500 (1971).
34. Knozinger, H., and Krietenbrik, H., *J. Chem. Soc. Faraday Trans. 1* **72,** 2421 (1976).
35. Sobalik, Z., Pour, V., Sokalova, L., Nevskaya, O., and Popova, N., *React. Kinet. Catal. Lett.* **31,** 297 (1986).
36. Tsyganenko, A., Pozdnyakov, D., and Filimonov, V., *J. Mol. Struct.* **29,** 299 (1975).
37. Busca, G., Saussey, H., Saur, O., Lavalley, J., and Lorenzelli, V., *Appl. Catal.* **14,** 245 (1985).
38. Dines, T., Rochester, C., and Ward, A., *J. Chem. Soc. Faraday Trans. 1* **87**(10), 1611 (1991).
39. Belokopytov, Y., Kholyavenko, K., and Gerei, S., *J. Catal.* **60,** 1 (1979).
40. Kantcheva, M., Hadjiivanov, K., and Klissurski, D., *J. Catal.* **134,** 299 (1992).
41. Andersson, A., *J. Catal.* **69,** 465 (1981).
42. Miyata, H., Fujii, K., Ono, T., Kubokawa, Y., Ohno, T., and Hatayama, F., *J. Chem. Soc. Faraday Trans. 1* **83,** 675 (1987).
43. Roozeboom, F., Mittelmeijer-Harzeger, M., Moulijn, J., Medema, J., de Beer, V., and Gellings, P., *J. Phys. Chem.* **84,** 2783 (1980).
44. Griffith, W., and Lensniak, P., *J. Chem. Soc. A,* 1066 (1969).
45. Went, G. T., Leu, L. J., Rosin, R. R., and Bell, T. A., *J. Catal.* **134,** 492 (1992).
46. Vuurman, M. A., and Wachs, I. E., *J. Phys. Chem.* **96,** 5008 (1992).
47. Tarama, K., Yoshida, S., Ishida, S., and Kakioka, H., *Bull. Chem. Soc. Jpn.* **41,** 2840 (1968).
48. Sanati, M., and Andersson, A., *J. Mol. Catal.* **59,** 233 (1990).
49. Centi, G., Pinelli, D., and Trifiro, F., *J. Mol. Catal.* **59,** 221 (1990).
50. Cavani, F., Centi, G., Parrinello, F., and Trifiro, F., *in* "Preparation of Catalysts IV" (B. Delmon, P. Grange, A. Jacobs, and G. Poncelet, Eds.), p. 227. Elsevier, Amsterdam, 1987.
51. Cavani, F., Centi, G., Foresti, E., Trifiro, F., and Busca, G., *J. Chem. Soc. Faraday Trans. 1* **84,** 237 (1988).
52. Andersson, S. L. T., *Catal. Lett.* **7,** 351 (1990).
53. Nakamoto, K., "Infrared and Raman Spectra of Inorganic and Coordination Compounds," Wiley, New York, 1978.
54. Tretyakov, N., and Kilimonov, V., *Kinet. Katal.* **14,** 803 (1973).
55. Sobalik, Z., Pour, V., Sokalova, L., Nevskaya, O., and Popova, N., *React. Kinet. Catal. Lett.* **30,** 179 (1986).